PAPER

Check for updates

A chitosan-based biopolymer as an encapsulating nanomaterial for enhancing the antifungal and aflatoxin B₁ inhibitory efficacy of *Zanthoxylum alatum* (Roxb) essential oil and elucidation of the mode of action

Amrita Yadav,[ab] Tanya Singh Raghuvanshi[a] and Bhanu Prakash [ID] *[a]

The study reports the green synthesis of nanoencapsulated *Zanthoxylum alatum* (Roxb) essential oil (Ne-ZAEO) using chitosan biopolymer and its assessment as an antifungal agent against food-borne molds and aflatoxin B₁ (AFB₁) contamination. Phytochemical analysis of essential oil (ZA-EO) was conducted by gas chromatography-mass spectroscopy (GC-MS). The fabricated Ne-ZAEO was analysed for average size (30−50 nm by scanning electron microscopy and atomic force microscopy), functional group interaction (Fourier transform infrared spectroscopy), and nature of crystallinity (X-ray diffraction). The Ne-ZAEO exhibited considerable encapsulation efficiency (37.33%) and loading capacity (6%). The *in vitro* minimum inhibitory concentration (MIC) of free ZAEO and Ne-ZAEO against *Aspergillus flavus* was found to be $1.20~\mu\text{L mL}^{-1}$ and $1.0~\mu\text{L mL}^{-1}$ respectively. The antifungal mechanism was linked to cellular dysfunction including ergosterol content, ion leakage, and carbon source utilization. In addition, the antioxidant activity (IC₅₀ value $59.93~\mu\text{L mL}^{-1}$) of Ne-ZAEO was explored using 2,2-diphenyl-1-picrylhydrazyl (DPPH). Ne-ZAEO at $1.0~\mu\text{L mL}^{-1}$ significantly protects the *Vigna unguiculata* legume seed samples from *A. flavus* growth and AFB₁ contamination and preserves its sensory characteristics. The study reports that Ne-ZAEO could be used as a green antifungal agent to protect food-grains from molds and AFB₁ contamination and extend their shelf-life.

Sustainability spotlight

The study reports new insights for the potential application of nanoencapsulated *Zanthoxylum alatum* (Roxb) essential oil (Ne-ZAEO) as a green antifungal agent against mold growth and aflatoxin B₁ contamination in agricultural food products.

1. Introduction

Mycotoxin contamination is one of the major reasons for the deterioration of the quality of food products, and often has negative health effects. Among all forms of mycotoxins, aflatoxin B₁ (AFB₁) contamination produced by food-borne molds, mainly by *Aspergillus flavus* and *Aspergillus parasiticus* is the most significant form with respect to incidence and toxicity.[1] The International Cancer Agency listed AFB₁ as a group 1 carcinogen with reported carcinogenic, teratogenic, immuno-suppressive, and hepatotoxic effects.[2] The literature review revealed that AFB₁ is approximately 68 times more toxic than arsenic and second only to botulinum.[3] Therefore, it is of great interest to reduce aflatoxin B₁ contamination in agri-food commodities and their finished products.

Over the decades, the massive and indiscriminate uses of synthetic antifungal agents induced fungicide resistance, and imposed negative effects on human and non-target species.[4,5] In this context, industries are looking for green chemicals, especially traditionally used plant-derived chemicals for efficient control of molds and AFB₁ contamination. Among plant products, essential oils (EOs) of aromatic plants harbour tremendous biological activity against a range of food-borne pathogens.[5,6] In general, EOs contains a variety of volatile and lipophilic compounds such as terpenes, terpenoids, phenylpropenes, ketones and phenolics, with strong odor, which often targeted the different cellular and metabolic processes of microbes and disturbed their homeostasis, thereby inhibiting their growth and proliferation.[5] The antifungal activities of essential oils were correlated with their diverse chemical profiles and synergistic effects among the functional groups.

[a]Department of Botany, Institute of Science, Banaras Hindu University, Varanasi, 221005, India. E-mail: bprakash@bhu.ac.in; bhanubhu08@gmail.com; Tel: +91-9794113055

[b]Smt. Indira Gandhi Govt. PG College, Lalganj, Mirzapur, Uttar Pradesh, India

Thus, in order to address the emergence of resistance among the targeted microbes, EOs could be used over conventional chemical fungicides with multi-targeted effects. *Zanthoxylum alatum* (Roxb), is an aromatic plant of the family Rutaceae, listed in the generally recognised as safe (GRAS) category by the US-FDA, and exhibits a wide range of bioactivities such as stomachic, carminative, disinfectant, and antiseptic, and has been used in traditional medicine systems in India and China for the treatment of fever, dyspepsia, cholera, and general debility.[7–9] Furthermore, the EO of *Zanthoxylum alatum* exhibited potent antimicrobial and antioxidant activity.[7,10]

Unfortunately, the interest in EO-based food preservatives has steadily declined in the last decade due to the loss of their biological activity during practical application often related to their volatile nature and negative interaction with the sensory characteristics of applicable food products. However, the recent nanoencapsulation technology could overcome these obstacles and provide a feasible and effective path to improve their physical stability, shielding them from interactions with food products with enhanced bioactivity due to the sub cellular size.[5,11] Nanoencapsulation of essential oils and their bioactive volatile compounds protects them from oxidation, volatility loss, adverse interaction with the food matrix (nutrient, water activity and pH) and preserves the organoleptic properties (flavour, odour, colour, and taste) with improved stability and controlled release in food products.[5]

Chitosan (linear polysaccharide of (1–4)-linked 2-amino-deoxy-β-D-glucan) is the second most prevalent natural polysaccharide after cellulose, exhibiting remarkable biocompatibility and antimicrobial activity.[5,12] Over the last decade, chitosan has been used as a fascinating polymer in drug delivery systems due to its low toxicity, biodegradability, and film-forming properties.[5]

Therefore, an investigation was carried out to explore the potential of low molecular weight chitosan biopolymers as an encapsulating wall material for chemically characterized *Zanthoxylum alatum* essential oil (ZAEO) to boost its antifungal aflatoxin B_1 inhibitory efficacy. The fabricated nanoencapsulated (Ne-ZAEO) was characterized by scanning electron microscopy (SEM), atomic force microscopy (AFM), Fourier transform infrared spectroscopy (FTIR), and X-ray diffraction (XRD) analysis. In addition, the antioxidant activity, probable mode of action and *in situ* efficacy (*Vigna unguiculata* model food system) against the toxigenic *Aspergillus flavus* and aflatoxin B_1 contamination have been investigated.

2. Materials and methods

2.1. Chemicals and equipment

The chemicals used in the study were of analytical grade and purchased from Hi-Media Laboratories Pvt Ltd, Mumbai, Sigma Chemical Co. (St. Louis, MO), USA, and Sisco Research Laboratory Pvt. Ltd, Mumbai, India. A hydro-distillation unit (Merck Specialities Pvt. Ltd, Mumbai, India), gas chromatograph-mass spectrometer (PerkinElmer, Turbomass Gold, USA), atomic absorption spectrophotometer (PerkinElmer, Analyst 800, USA), spectrophotometer from Shimadzu (UV-1800), cooling

centrifuge (CPR-24 plus, Remi), probe-type sonicator (Labman Scientific instrument, Pro-500), lyophilizer (Christ, alpha D plus, Australia), scanning electron microscope (Evo-18 researcher, Zeiss), Fourier transform infrared spectrometer (PerkinElmer, USA) and X-ray diffractometer (Bruker D8 Advance) were used in the study.

2.2. Extraction of ZAEO and qualitative analysis of its chemical profile by GC-MS

The seed samples of *Zanthoxylum alatum* (Roxb) (ZA) were procured from the Varanasi district of the state of Uttar-Pradesh, India. The extraction of essential oil was performed by using Clevenger's apparatus for a period of 5 h at 90 °C. After 5 h the essential oil was collected in a clean and sterilized glass vial and the droplets of H_2O were removed by adding 10 mg of anhydrous Na_2SO_4.[13] Thereafter, the chemical profiling of the various aromatic compounds present in EO was conducted by GC-MS analysis. The separation conditions were set as per the following: elite-5 capillary column (column length = 30 m, inner diameter = 0.25 mm, film thickness = 0.25 mm), oven: initial temp 80 °C for 2 min, ramp 10 °C min^{-1} to 250 °C, hold 10 min, inj = 250 °C, split = 20 : 1, carrier gas = He, solvent delay = 2.00 min, transfer temp = 180 °C, source temp = 160 °C, scan: 40–400 Da. The injection volume 1 μl (1 : 100 dilution in acetone) and compounds were identified based on their spectral pattern available in the literature Wiley, and the NIST library.[14]

2.3. Synthesis of the nanogel and encapsulation of ZAEO

The encapsulating wall material (chitosan-based nanogel) was prepared using low molecular weight chitosan, cinnamic acid, and zero length cross linker *N*-(3-dimethylaminopropyl)-*N*-ethylcarbodiimide hydrochloride (EDC) based on a previously described protocol by Beyki *et al.* (2014)[15] with minor modifications. In the first step, the stock solution (A) was prepared by dissolving chitosan (0.5 grams) in 1% aqueous acetic acid (w/v) solution until the solution was transparent under magnetic stirring at 400 rpm. Subsequently, 85 mL methanol was slowly poured into stock solution (A) under continuous stirring conditions of 250 rpm for 30 minutes at room temperature followed by sonication for a duration of 10 minutes at acidic pH (3.5–4). Thereafter, stock solution (B) was prepared containing EDC (669 μL) and cinnamic powder (317.5 mg), and 75 mL of stock solution A was added to this and kept for a day under continuous stirring conditions (250 rpm). The pH of the solution was then adjusted to basic (pH 8.5–9.00) using NaOH pellets to precipitate the nanogel. The nanogel was centrifuged at 9000 rpm for 15 min to recover the nanogel precipitate followed by gentle washing with distilled water and ethanol (4–6 times). Thereafter, the nanogel precipitate was dried under vacuum for 24 hours, and the lyophilized nanogel was then resuspended in 0.1% acetic acid under magnetic stirring until the pH becomes acidic (3.5–4). To obtain the desired concentration of chitosan and ZAEO (w/w) (1 : 0, 1 : 0.25, 1 : 0.50, 1 : 0.75, and 1 : 1.0), different doses of ZAEO were added to the prepared nanogel and sonicated at (50 Hz for 30 min) using a probe-type sonicator to obtain the nanorange particle size.

2.3.1 Encapsulation efficiency and loading capacity.

Encapsulation efficiency and loading capacity were figured out by following the method described by Hosseini *et al.* (2013)[16] using a UV-vis spectrophotometer. The percentage of ZAEO encapsulated inside the chitosan-based nanoparticle was assessed at 208 nm (absorption maximum of ZAEO) by using a UV-vis spectrophotometer. The percent (%) encapsulation efficiency and % loading capacity were calculated using a standard curve ($R^2 = 0.998$) from mathematical formulations 1 and 2 respectively.

$$\% \text{ Encapsulation efficiency (\% EE)} = (\text{Mass of loaded ZAEO})/(\text{Mass of initial ZAEO}) \times 100$$

$$\% \text{ Loading capacity (\% LC)} = (\text{Total amount of loaded ZAEO})/(\text{Weight of the freeze-dried sample}) \times 100$$

2.3.2 Characterization of Ne-ZAEO

2.3.2.1 SEM and AFM investigation. Scanning electron microscopy (SEM) and atomic force microscopy (AFM) techniques were employed to investigate the size, shape, and height of the synthesized Ne-ZAEO. Briefly, 10 μL of ultrasonicated nanogel and nanogel with ZAEO was dripped on a sterilised cover slip, and a thin layer was prepared and air dried. The dried thin film of nanoparticles was gold coated under high vacuum and analyzed at various magnifications under a SEM (Evo-18 researcher, Zeiss) and AFM (Atomic force microscopy, NT-MDT).[17]

2.3.2.2 FTIR analysis. Detection of functional groups and the type of covalent interaction of ultrasonicated (15 min) samples of pure chitosan, ZAEO, and chitosan–cinnamic acid nanoparticles and Ne-ZAEO was carried out by Fourier transform infrared spectroscopy (FTIR) (PerkinElmer) using KBr pellets at a vibrational frequency ranging from 400 to 4000 cm^{-1}.

2.3.2.3 X-ray diffraction (XRD) analysis. The low molecular weight chitosan, chitosan–cinnamic acid nanogel, and Ne-ZAEO were analyzed using an X-ray diffractometer (Bruker D8 Advance) in the 2θ range of 5–60° with a steep angle of 0.02° min^{-1} and a scan speed of 5° min^{-1} to assess the crystalline or amorphous nature of the material.

2.4. Minimum inhibitory concentration (MIC) of ZAEO and Ne-ZAEO against selected food-borne molds and aflatoxin B₁ production: *in vitro* assay

The minimum inhibitory concentration (the doses at which no noticeable growth of test molds was observed) of free and nanoencapsulated ZAEO has been recorded using the poisoned food technique following Prakash *et al.* (2012 b).[18] Briefly, different doses of (0.2–2.0 μL mL^{-1}) of ZAEO and Ne-ZAEO were diffused separately in 0.5 mL tween-20, followed by the PDA medium in Petri-dishes; thereafter, 5 mm discs of test mold species *Aspergillus flavus*, *Aspergillus niger*, *Aspergillus fumigatus*, *Aspergillus luchuensis*, *Aspergillus repens*, *Aspergillus terreus*, *Penicillium italicum*, *Fusarium oxysporum*, *Curvularia lunata*, *Alternaria alternata*, and *Rhizopus stolonifer* were placed im the

center and kept in a BOD incubator for 7 days. After incubation, the Petri-plates where no visible growth was observed were considered as MIC.

For aflatoxin B₁ inhibitory efficacy different doses of (0.2–1.2 μL mL^{-1}) ZAEO and Ne-ZAEO were diffused separately in 0.5 mL tween-20 in a flask containing 24.5 mL SMKY (sucrose, 200 g; MgSO4·7H₂O, 0.5 g; KNO₃, 0.3 g and yeast extract, 7 g; 1000 mL distilled water) medium, and each flask was separately inoculated with a 50 microliter spore suspension of the toxigenic strain of *A. flavus*, followed by incubation for 10 days in a BOD incubator at 27 ± 2 °C. After the provision period, the media was filtered and the filtrate was used for the estimation of AFB₁ content in the liquid medium following the previously described method without any modification.[13] The amount of AFB₁ was calculated based on the optical density of the supernatant using the formula:

$$\text{AFB}_1 \text{ content (μg mL}^{-1}) = (D \times M)/(E \times L) \times 1000$$

where *D*, absorbance; *M*, the molecular weight of AFB₁ (312); *E*, the molar extinction coefficient of AFB₁ (21 800); *L*, path length (1 cm cell was used).

2.5. Mechanism of action

2.5.1 Effect of Ne-ZAEO on cell membrane integrity (ergosterol and membrane cation leakage).

The extraction and quantification of ergosterol in the cell membrane of *A. flavus* exposed to different doses of Ne-ZAEO were performed according to Tian *et al.* (2012).[19] Briefly, different doses of Ne-ZAEO (0.2–1.0 μL mL^{-1}) were prepared in the SMKY medium, followed by addition of a 50 μL spore suspension of *A. flavus*. The flasks were then incubated for five days in a BOD incubator. After that, biomass was harvested, dried, weighed and transferred to sterile borosilicate glass tubes, followed by addition of 5 mL of newly formed 25% alcoholic potassium hydroxide solution (25 g of KOH and 35 mL of sterile water, brought to 100 mL with 100% ethanol). The flasks were kept on vortex agitation for 2–5 min and incubated in a water bath at 85 °C for 3 h, and the tubes were allowed to cool to room temperature. Then sterols were extracted by addition of a mixture 5 mL *n*-heptane and 2 mL sterile distilled water. The heptane phase was transferred to a clean glass tube. The optical density of the *n*-heptane layer was analyzed (230 and 300 nm) for the quantification of ergosterol using the given mathematical equation.

$$\% \text{ Ergosterol} = \left(\frac{A_{282}/290}{\text{Pellet Weight}}\right) - \left(\frac{A_{230}/518}{\text{Pellet Weight}}\right)$$

$$\% \text{ Ergosterol} + \% \text{ 24(28)} - \text{dehydroergosterol} = \frac{A_{282}/290}{\text{Pellet Weight}}$$

$$\% \text{ 24(28)} - \text{dehydroergosterol} = \frac{A_{230}/518}{\text{Pellet Weight}}$$

where 290 and 518 are *E* values in percentages per cm determined for crystalline ergosterol and 24(28) dehydroergosterol.

2.5.2 Effect of Ne-ZAEO on membrane cation efflux. Efflux of vital cellular cations such as Ca^{2+}, K^{+} and Mg^{2+} ions was measured according to the method of Helal *et al.* (2007).[20] For the accomplishment of this methodology, initially *A. flavus* was cultured in SMKY growth media, and five days old *A. flavus* biomass was suspended in 20 mL of 0.85% saline solution and then treated with different doses of half MIC, MIC, and double MIC (0.5, 1.0, and 2.0 μL mL^{-1}) of Ne-ZAEO and kept for a 12 h incubation period at room temperature. After incubation, the biomass was harvested and the filtrate was used to release Ca^{2+}, K^{+}, and Mg^{2+}ions using atomic absorption spectrometry.

2.5.3 Effect of Ne-ZAEO on carbon source utilization. The carbon source consumption pattern of NeZAEO was assessed following the method of Singh (2009)[21] using a Biolog FF Microplate (94545, Hayward, CA). For this, five days old *A. flavus* grown on a PDA medium (9.5 mL) in Petri-plates was exposed to the desired concentration of Ne-ZAEO (0.5, 1.0, and 2.0 μL mL^{-1}) and kept for an incubation period (four days at 27 ± 2 °C). The Petri plate without ZAEO served as the control. After incubation, fungal spores from both control and treatment sets were isolated with sterile cotton swabs and mixed into FF-inoculating fluid with adjusted transmittance (75%) using a turbidometer. Thereafter, 100 μL FF-inoculating fluid was dropped in the wells of FF Micro-Plates and kept in a BOD incubator for 24 h. The absorbance was measured at 490 nm using a Biolog plate reader (Biolog, ELx808BLG, Biotek Instrument USA). Percent inhibition in various C-sources in *A flavus* exposed to Ne-ZAEO was calculated over the control.

2.6. Antioxidant activity of ZAEO and Ne-ZAEO through DPPH free radical assay

The free radical scavenging activity of ZAEO and Ne-ZAEO was analyzed using DPPH free radicals following the methods of Prakash *et al.* (2012).[10] Briefly, the desired amounts of ZAEO and Ne-ZAEO were added to 4 mL of methanolic solution of DPPH (0.004%), and then the mixture was left at room temperature for 30 min in the dark. The absorbance of the aliquot was measured at 517 nm by using a spectrophotometer. The percent inhibition (IC_{50} value) was described by using the graph plotted with the concentration of test samples and scavenging rate of DPPH free radicals with respect to those of the blank calculated using the formula where A = absorbance.

$$\% \text{ Inhibition} = [(A_{blank} - A_{sample})/A_{blank}] \times 100$$

2.7. Assessing the antifungal and aflatoxin B₁ inhibitory effect of Ne-ZAEO on the food system (*Vigna unguiculata*) and its effect on sensory properties: *in situ* observation

To investigate the practical application of Ne-ZAEO, the legume seed of *V. unguiculata* was selected as a model food system. Briefly, 500 g seed samples were placed inside a 2.5 L plastic jar previously inoculated with a 500 μL of toxigenic *A. flavus* spore suspension (10^{6} spore per ml) in each jar. Thereafter, each jar was fumigated with 1.0 μL mL^{-1} of Ne-ZAEO and incubated for

6 months at the laboratory. After incubation, the level of fungal contamination was examined by the direct plating and serial dilution method, while aflatoxin B₁ content was measured by HPLC, using the standard curve ($Y = 2545.7 \times -81\,275$, $R^2 = 0.9602$) following Kedia *et al.* (2015).[22] Moreover, sensory properties of *Vigna unguiculata* seed samples exposed to Ne-ZAEO at 1.0 μL mL^{-1} (six months) were investigated by a panel of ten expert personnel on the basis of a 9-point scale for color, odor, texture, and overall acceptability with respect to the control sets (9 = like extremely, 8 = like very much, 7 = like moderately, 6 = like slightly, 5 = neither like nor dislike, 4 = slightly dislike, 3 = moderately dislike, 2 = very much dislike, and 1 = extremely dislike).

2.8. Statistical analysis

The experiments were performed in triplicate (mean ± SE). The results were subjected to a one-way analysis of variance (P values of ≤0.05) and Tukey's multiple-range tests to identify significant differences in the comparison of means using SPSS program version 16.0 for Windows (SPSS Inc., IBM Corp).

3. Results and discussion

3.1. Extraction and chemical profile of ZAEO

Essential oil (yield 1.5 %v/w) was extracted from the seeds of *Zanthoxylum alatum* (Roxb.) using the hydro-distillation apparatus and its chemical profile was analyzed using GC-MS analysis. The result revealed the presence of thirteen different bioactive components, accounting for 95.23% of the total essential oil composition. The identified phytochemicals, retention time, and percentage are presented in Table 1 and Fig. 1. GC-MS analysis also confirms that cineol (46%) is a major bioactive component followed by D-limonene (16.73%) and linalool (12.67%). The literature review reports that variation in the chemical profile (often due to the differences in the harvest season, geography, plant populations, and edaphic factors) may significantly alter the biological activity of essential oils against the targeted microbes; hence, in the present investigation, prior

Table 1 GC-MS analysis of *Zanthoxylum alatum* essential oil (ZAEO)

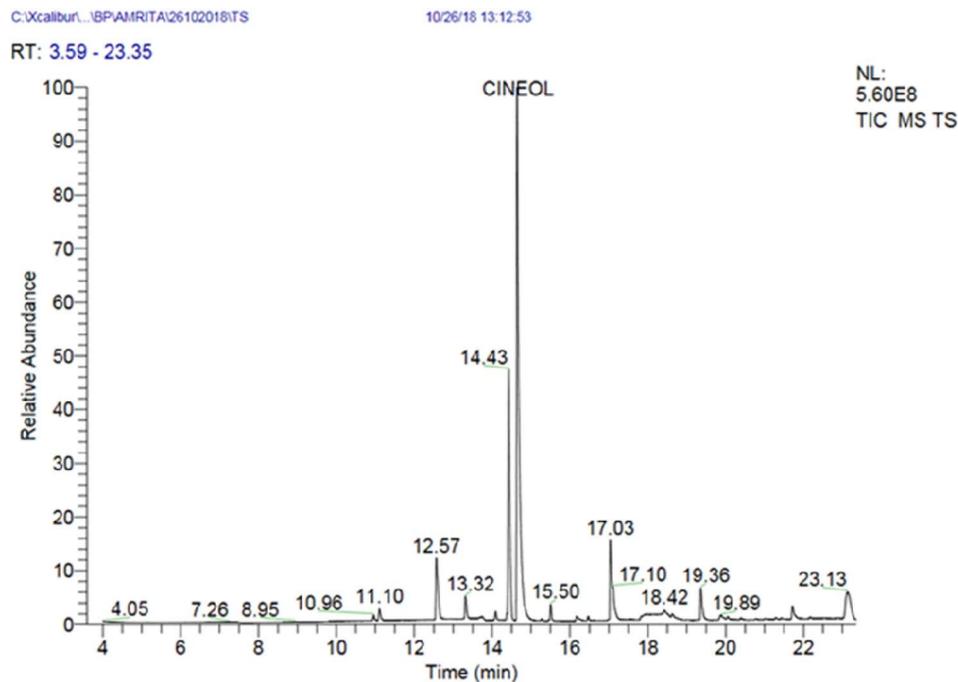| S. no	Compounds	Retention time	Percentage (%)
1	β-Thujene	10.96	0.13
2	4(10)-Thujene	12.57	5.18
3	α-Pinene	13.32	1.04
4	D-Limonene	14.43	16.73
5	Cineol	14.64	46.11
6	Gamma-terpinene	15.5	0.41
7	Terpinolene	16.17	3.44
8	Linalool	17.03	12.67
9	Terpinen-4-ol	19.36	2.91
10	Estragole	20.05	6.08
11	Cumaldehyde	21.28	0.06
12	L-Carvone	21.44	0.04
13	Piperitone	21.71	0.43
		Total	95.23

Fig. 1 GC-MS chromatogram of *Zanthoxylum alatum* essential oil (ZAEO).

to nanoencapsulation and further assessment on antifungal efficacy, the ZAEO was characterised by GC-MS.[10,23]

3.2. Preparation of chitosan–cinnamic acid nanoparticles and nanoencapsulation of ZAEO, and its characterization

Chitosan (*N*-acetyl derivative of chitin), is one of the widely used encapsulating wall materials in food and bioengineering industries for encapsulation of active food ingredients and various phytochemicals. Chitosan along with cinnamic acid and EDC (zero-length cross-linker) show favourable nature for the chitosan nanogel synthesis. The synthesized nanogel forms two layers, an outer hydrophilic layer and an inner hydrophobic cavity or cage-like structure which often traps EOs.[15,24,25] The different doses of ZAEO were loaded inside the synthesized nanogel followed by an ultrasonication process using a probe sonicator, leading to the entrapment of ZAEO inside the self-organized hydrophobic cavity. The percentage encapsulation efficiency (% EE) and loading capacity (% LC) of the chitosan–cinnamic acid-based nanogel was determined using UV-vis spectrophotometry at 208 nm, the absorbance maxima of ZAEO. The maximum percentage encapsulation efficiency (% EE) and percentage loading capacity (% LC) of ZAEO were recorded at a chitosan/ZAEO (w/w) ratio of 1 : 0.50, and was found to be 37.33% and 6%, respectively. This observation was in accordance with the previous study available in the literature. Xu *et al.* (2023)[26] reported that the EE and LC of clove EO inside the chitosan nanogel ranged from 39.0 and 15.43. Mondejar-Lopez *et al.* (2022)[27] reported the maximum EE (32.8) and LC (19.8) of garlic EO in the chitosan nanogel. Furthermore, the literature review reported that the variation in EE and LC can be significantly attributed to varied EO composition, loaded

amount, synthesis process of wall material, nanoparticle shape, size, and dispersity.[26,28]

3.2.1 Characterization of Ne-ZAEO. The characterization of the fabricated Ne-ZAEO was further analyzed for average size (23–50 nm by scanning electron microscopy and atomic force microscopy) functional group interaction (Fourier transform infrared spectroscopy), and crystallinity nature (X-ray diffraction).

Scanning electron microscopy (SEM) and atomic force microscope (AFM) images revealed that the chitosan nanogel and Ne-ZAEO present spherical shapes with an average size ranging between 23–50 nm as shown in Fig. 2a–d. The nearly spherical, smooth and nano-range of synthesised Ne-ZAEO could facilitate the control and effective release of ZAEO during its application in food systems because of large surface area. In addition, the nanoencapsulation also provides the stability to ZAEO by protecting it from the external environment such as temperature, humidity and light and possible adverse interaction with food matrix (nutrient, water activity and pH).[5] Moreover, FTIR spectra of chitosan powder, chitosan cinnamic acid nanogel, ZAEO, and Ne-ZAEO are shown in Fig. 3A–D. Fig. 3 shows that the FTIR absorption bands for chitosan show several characteristic peaks at 3437 cm^{-1} (–OH/–NH$_2$ functional group), 1628 cm^{-1} (amino group), and 1031 cm^{-1} (C–O–C stretching). The spectra obtained for the chitosan cinnamic acid nanogel also exhibited similar major peaks at 3444 cm^{-1} (–OH and –NH$_2$ stretching) and 1639 cm^{-1} (–CO stretching). More specifically, the chitosan cinnamic acid-dependent nanogel formulation was confirmed through the appearance of covalent bonding (amide linkage) at 1639 cm^{-1} between the –NH (amino) group of chitosan and –COO (carboxyl) group of cinnamic acid. The
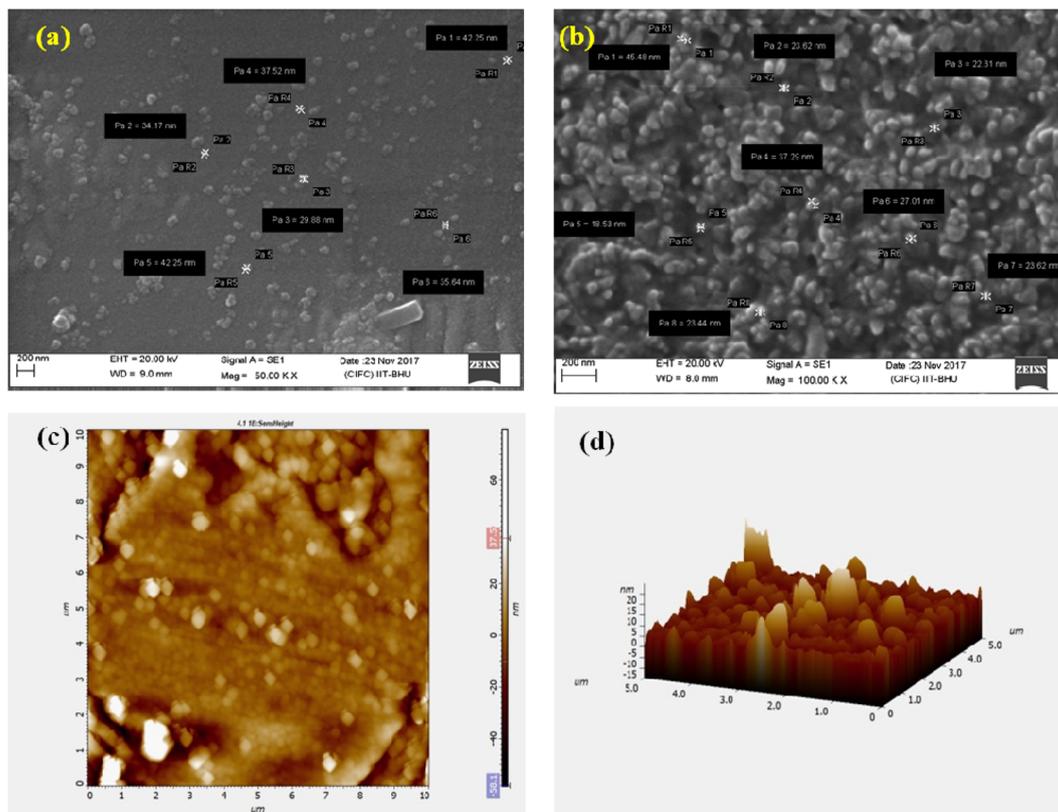
Fig. 2 SEM images of (a) chitosan–cinnamic acid nanoparticles and (b) nanoencapsulated ZAEO (Ne-ZAEO) and AFM of Ne-ZAEO: (c) 2D image and (d) 3D image.
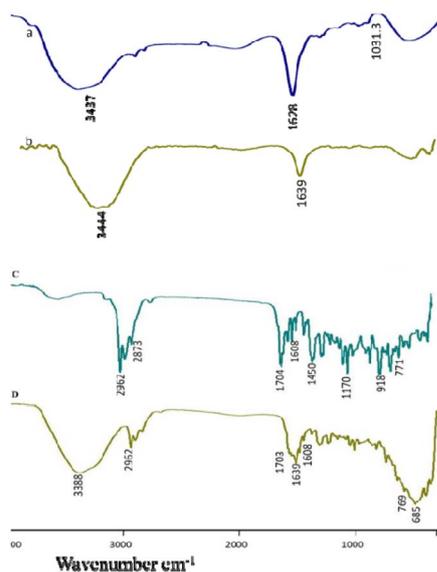

Fig. 3 FTIR spectra of (A) chitosan, (B) the chitosan–cinnamic acid nanogel, (C) *Zanthoxilum alatum* EO (ZAEO) and (D) Ne-ZAEO.

ZAEO retained most of the peaks present in the spectra of ZAEO with a slight shift in the wave number. Thus, FTIR characterization reflects that there was a positive interaction between the ZAEO and nanogel, presumably due to the larger number of hydrophobic interactions. Fig. 4 depicts the graphical presentation of low molecular weight chitosan, the chitosan–cinnamic acid-based nanogel and the nanogel packed with ZAEO obtained from XRD diffractograms. The chitosan powder exhibited a high extent of crystallinity with sharp peaks at 2θ values of 10.8° and 20.9°; however, the degree of amorphousness was increased after interaction between ZAEO and yje nanogel. Payandeh *et al.* (2022)[29] reported a disarray in crystallinity of chitosan attributed to the molecular interaction between chitosan and cinnamic acid and functional groups of essential oils. FTIR analysis and XRD analysis of chitosan, the
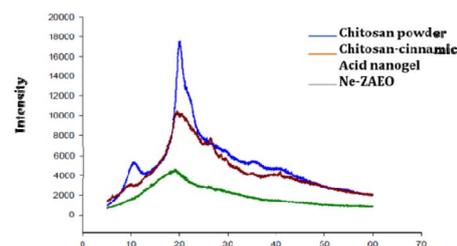
characteristic peaks of ZAEO are at 2962 cm^{-1}, 2873 cm^{-1}, 1704 cm^{-1}, 1608 cm^{-1} (–CO stretching), 1450 cm^{-1} (–NH bending and –CN stretching), 1170 cm^{-1} (aromatic C–H in plane bend), 918 cm^{-1} and 771 cm^{-1} (out of plane –NH bending). Ne-

Fig. 4 X-ray diffractogram: (A) chitosan, (B) the chitosan–cinnamic acid nanogel and (C) Ne-ZAEO.

chitosan cinnamic acid nanogel and NE-ZAEO exhibited close agreement with published ones.[30,31]

3.3. Antifungal and anti-aflatoxigenic activity: *in vitro* assay

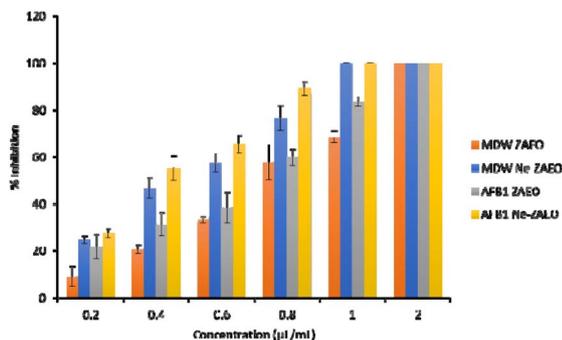The antifungal and aflatoxin B_1 inhibitory activity of ZAEO and Ne-ZAEO was analyzed and reported in terms of minimum inhibitory concentration (MIC) against the toxigenic species of *A. flavus*. The MIC for growth and aflatoxin B_1 inhibition of ZAEO and Ne-ZAEO was found to be 1.2 µL mL^{-1} and 1.0 µL mL^{-1}, respectively, as shown in Fig. 5. In addition, the efficacy of ZAEO and Ne-ZAEO against the selected food-borne molds are shown in Fig. 6. The results show that Ne-ZAEO exhibited superior activity over the free form as it required low doses for mold growth and AFB_1 inhibition, which could be due to the decrease in particle size, leading to the increase in the surface-to-volume ratio, controlled release at the site of action, and cumulative effects of ZAEO and chitosan due to interaction between the positively charge chitosan and negatively charged fungal cell wall and membrane.[32,33] The results were consistent with the available literature, which revealed that the nano-encapsulation of essential oils and their volatile compounds such as *Zataria multiflora*, *Satureja kermanica*, Citral and cinnamaldehyde exhibited enhanced efficacy against molds under both *in vitro* and *in situ* conditions.[29,34,35]

Fig. 5 Effect of ZAEO and Ne-ZAEO on MDW and AFB_1 production by *A. flavus* in the SMKY medium.
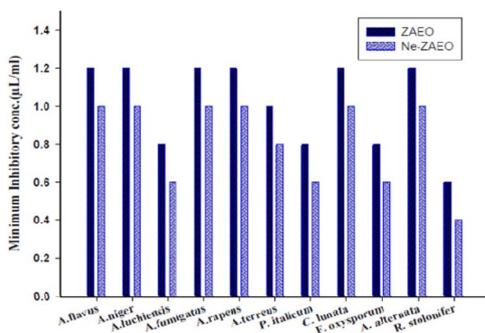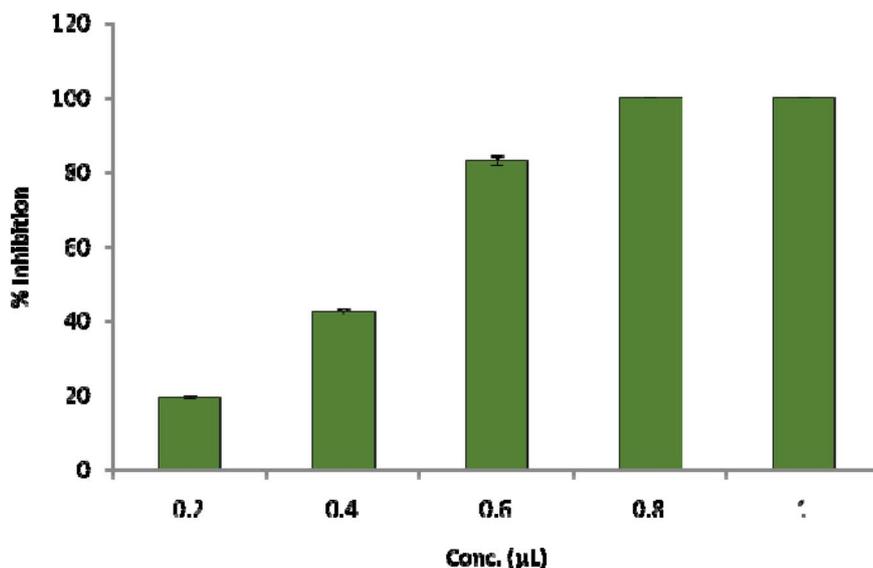

Fig. 6 Fungitoxic spectrum of ZAEO and Ne-ZAEO.

3.4. Antifungal and aflatoxin B_1 inhibitory mechanism of Ne-ZAEO

The result shows a significant reduction in ergosterol content with different concentrations of Ne-ZAEO. The reduction percentage of ergosterol content was found to be 19.26, 42.54, 83.06, and 100% at 0.2, 0.4, 0.6, and 0.8 µL mL^{-1} of Ne-ZAEO, respectively, in a dose-dependent manner as shown in Fig. 7. The ion leakage study based on AAS (atomic absorption spectroscopic) analysis also revealed an enhancement in the leakage of membrane cations (Ca^{2+}, K^+, and Mg^{2+}) with the increasing concentration of Ne-ZAEO compared with that of the control set as shown in Fig. 8. The lipophilic properties of the EO made its entry through the cell membrane easy, and leads to an impairment of the membrane integrity. Ergosterol, a 5,7-diene oxysterol, is the most abundant sterol in fungal cell membranes and is mainly responsible for regulating permeability,
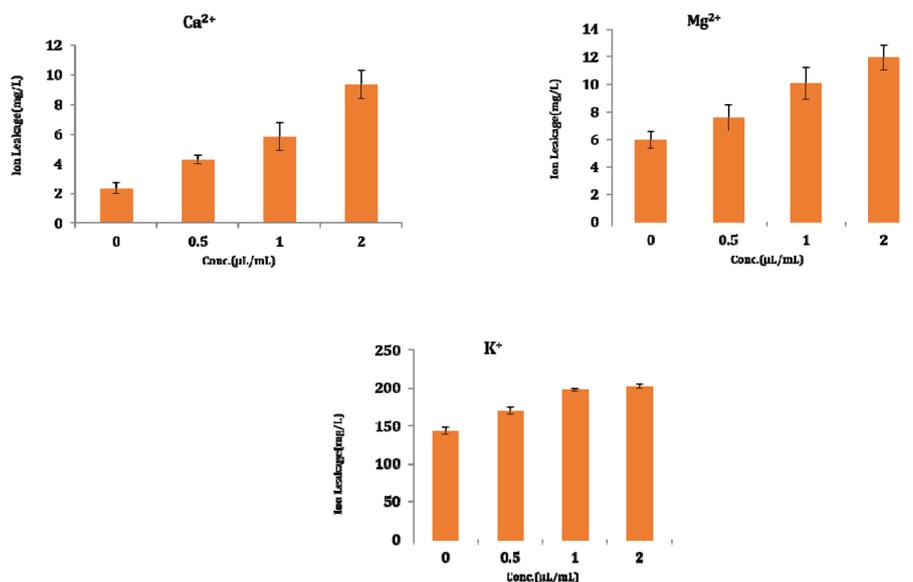

Fig. 7 Percent inhibition of ergosterol content.

Fig. 8 Membrane ion (Ca^{2+}, K^+ and Mg^{2+}) leakage from *A. flavus* cell fumigated with Ne-ZAEO.

protecting leakage of cellular contents, fluidity, and maintaining cellular homeostasis and is the prime target of the majority of available antifungal agents.[36,37] Hence, a decrease in ergosterol content may alter the membrane functioning, resulting in the extracellular release of vital cellular contents, which often participate in the development of fungal hyphal tips, thus leading to loss of vital cellular function required for cell growth.[38] The report emphasizes that the inhibition of ergosterol biosynthesis is one of the prime target sites of action of Ne-ZAEO. Furthermore, the utilization of carbon substrates is rudimentary for fungal cell growth and important vital cellular activities. The results of carbon substrate utilization fingerprints show that in the treatment sets, the decrease in utilization of different carbon sources such as D-arabinose, D-ribose, D-trehalose, L-arabinose, D-ribose, D-trehalose, D-xylose, maltotriose, sucrose, palatinose, and stachyose have been observed contrary to in the control set in *A. flavus* exposed to different

concentrations of Ne-ZAEO (at half MIC 0.5 µL mL^{-1} and MIC1.0 µL mL^{-1}) as shown in Fig. 9. Thus, it could be concluded that the decrease in C-source utilization in response to different doses of Ne-ZAEO may hamper the various metabolic pathways *viz* the pentose phosphate pathway (PPP), glycolysis and tricarboxylic cycle (TCA), lead to the significant suppression of the catabolic pathway, and interfere with cellular energy (ATP) generation, and thus influence the process of glycolysis resulting in inhibition of fungal cell growth and toxin production.[39,40] Hence, the study demonstrated that the plasma membrane impairment (ergosterol decrease and cation leakage) and change in the carbon source utilization pattern would be the prime cause for inhibition of growth of *A. flavus*.

3.5. Free radical scavenging activity of ZAEO and Ne-ZAEO

Free radical scavenging activity of ZAEO and Ne-ZAEO was explored using the DPPH method, one of the widely used
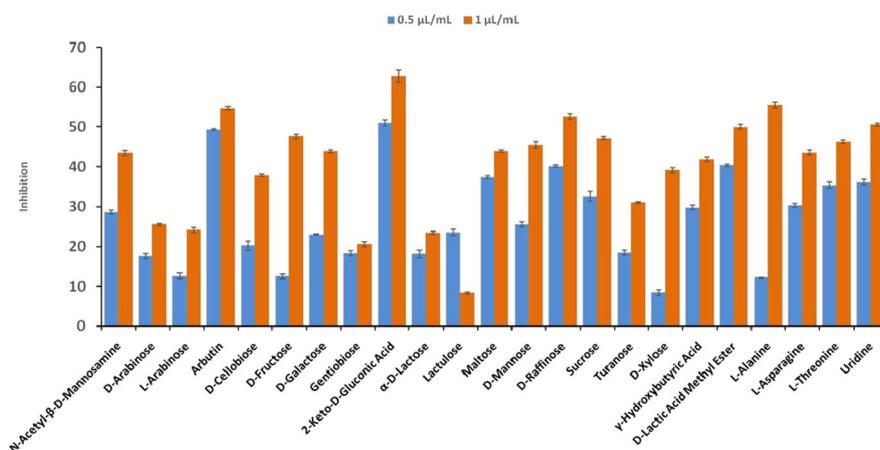

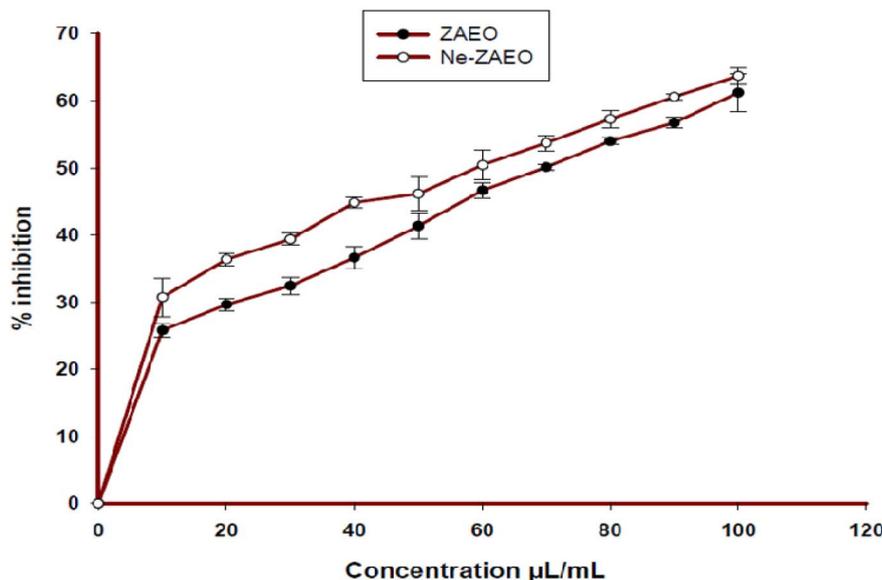Fig. 9 Inhibition of carbon source utilization by *A. flavus* fumigated with different doses of Ne-ZAEO.

Fig. 10 Percent radical scavenging activity of ZAEO and Ne-ZAEO through DPPH assay.

methods to assess the free radical scavenging effects of plant EOs. The IC_{50} value of free ZAEO and Ne-ZAEO to neutralize DPPH radicals was recorded to be 70.83 μL mL^{-1} and 59.93 μL mL^{-1}, respectively (Fig. 10). The nanoencapsulated EO (Ne-ZAEO) exhibited higher antioxidant activity compared to its free form. This might be a consequence of the cumulative positive effects during the interaction of ZAEO inside the nanogel. Thus, Ne-ZAEO could be used as a green preservative agent that possesses both antifungal and antioxidant activity to extend the shelf-life of food commodities.

3.6. Antifungal and aflatoxin B_1 inhibitory effects of Ne-ZAEO in the food system (*V. unguiculata*) and its effect on sensory properties: *in situ* observation

To investigate the *in situ* efficacy of Ne-ZAEO during the practical application, *Vigna unguiculata* seed samples were selected as a model food system. The results show that Ne-ZAEO exhibited considerable protection of *V. unguiculata* seed samples from *A. flavus* and AFB_1 contamination (Fig. 11).
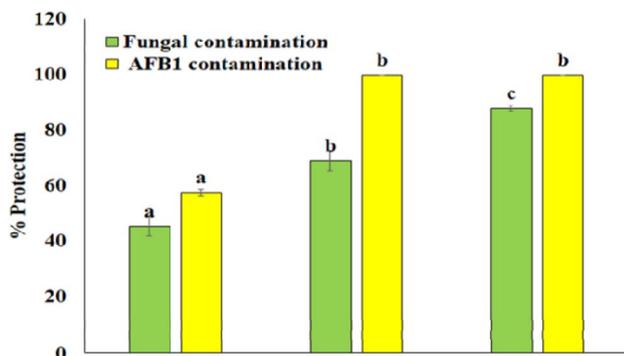

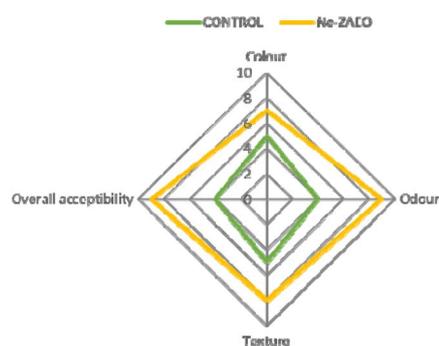Fig. 11 % Protection of *V. unguiculata* seed samples from *A. flavus* and AFB_1 contamination.

Fig. 12 Sensory analysis.

Furthermore, Ne-ZAEO effectively controls the negative effect of free ZAEO on the sensory characteristics (texture, odor, color, and overall acceptability) of model food at MIC doses (1.0 μL mL^{-1}) during up to six months of storage under laboratory conditions (Fig. 12). Contrary to this, the non-fumigated control set had lost the sensory (color, odor, texture, and overall acceptability) nature of *V. unguiculata* legume seed samples. Therefore, Ne-ZAEO could be used as a natural food preservative to enhance the shelf-life of stored food commodities after proper standardization of its doses.

4. Conclusion

The present study provides novel insights into the fabrication of ZAEO inside chitosan biopolymers and its potential application as a green plant-based antifungal and antioxidant agent. The nanoencapsulation of ZAEO inside the chitosan biopolymer exhibited remarkable encapsulation efficiency and loading capacity. Furthermore, the fabrication of ZAEO was characterized by SEM, AFM, FTIR, and XRD. Moreover, the fabricated Ne-

ZAEO was found to be more effective that its free form as it shows enhanced antifungal and aflatoxin B_1 inhibitory potential, and antioxidant efficacy. Furthermore, the antifungal mechanisms of action were found to be related to impairment in cellular functioning especially due to the perturbance in plasma membrane functioning and nutrient utilization associated with a decrease in ergosterol, increase in ion leakage, and carbon source utilization. During *in situ* application, Ne-ZAEO displays a significant protection of *V. unguiculata* seed samples against toxigenic *Aspergillus flavus* and aflatoxin B_1 contamination without any significant effects on its sensory characteristics. Thus, Ne- ZAEO could be used as a green antifungal agent to extend the shelf-life of agri-food products. However, further research warrants the improvement and optimization of encapsulation methods for high encapsulation efficiency, loading capacity, controlled release, cost-benefit ratio, prolonged safety and risk assessment of nano-encapsulated EOs on consumer health and nutritional composition of applicable food products during its industrial application.

Conflicts of interest

No potential conflict of interest was reported by the authors.

Acknowledgements

References

1 E. Pellicer-Castell, C. Belenguer-Sapina, P. Amoros, J. M. Herrero-Martinez and A. R. Mauri-Aucejo, Bimodal porous silica nanomaterials as sorbents for an efficient and inexpensive determination of aflatoxin M1 in milk and dairy products, *Food Chem.*, 2020, **333**, 127421.

2 Y. Chen, Q. Kong and Y. Liang, Three newly identified peptides from Bacillus megaterium strongly inhibit the growth and aflatoxin B1 production of Aspergillus flavus, *Food Control*, 2019, **95**, 41–49.

3 M. Kapustová, G. Granata, E. Napoli, A. Puškárová, M. Bučková, D. Pangallo and C. Geraci, Nanoencapsulated essential oils with enhanced antifungal activity for potential application on agri-food, material and environmental fields, *Antibiotics*, 2021, **10**(1), 31.

4 S. D. Nusair, M. J. Almasaleekh, H. Abder-Rahman and M. Alkhatatbeh, Environmental exposure of humans to bromide in the Dead Sea area: Measurement of genotoxicy and apoptosis biomarkers, *Mutat. Res., Genet. Toxicol. Environ. Mutagen.*, 2019, **837**, 34–41.

5 B. Prakash, A. Kujur, A. Yadav, A. Kumar, P. P. Singh and N. K. Dubey, Nanoencapsulation: An efficient technology to boost the antimicrobial potential of plant essential oils in food system, *Food Control*, 2018, **89**, 1.

6 B. Prakash, A. Kumar, P. P. Singh and L. S. Songachan, Antimicrobial and antioxidant properties of phytochemicals: Current status and future perspective, *Functional and Preservative Properties of Phytochemicals*, 2020, pp. 1–45.

7 N. Jain, S. K. Srivastava, K. K. Aggarwal, S. Ramesh and S. Kumar, Essential oil composition of Zanthoxylum alatum seeds from northern India, *Flavour Fragrance J.*, 2001, **16**(6), 408–410.

8 Y. Liu, Q. Li, W. Yang, B. Sun, Y. Zhou, Y. Zheng, M. Huang and W. Yang, Characterization of the potent odorants in Zanthoxylum armatum DC Prodr. pericarp oil by application of gas chromatography–mass spectrometry–olfactometry and odor activity value, *Food Chem.*, 2020, **319**, 126564.

9 https://www.accessdata.fda.gov/scripts/cdrh/cfdocs/cfcfr/cfrsearch.cfm?fr=182.20.

10 B. Prakash, P. Singh, A. Kedia and N. K. Dubey, Assessment of some essential oils as food preservatives based on antifungal, antiaflatoxin, antioxidant activities and *in vivo* efficacy in food system, *Food Res. Int.*, 2012, **49**(1), 201–208.

11 S. Gupta and P. S. Variyar, Nanoencapsulation of essential oils for sustained release: application as therapeutics and antimicrobials, in *Encapsulations*, Academic Press, 2016, pp. 641–672.

12 X. Zhang, B. B. Ismail, H. Cheng, T. Z. Jin, M. Qian, S. A. Arabi, D. Liu and M. Guo, Emerging chitosan-essential oil films and coatings for food preservation-A review of advances and applications, *Carbohydr. Polym.*, 2021, **273**, 118616.

13 B. Prakash, R. Shukla, P. Singh, P. K. Mishra, N. K. Dubey and R. N. Kharwar, Efficacy of chemically characterized Ocimum gratissimum L. essential oil as an antioxidant and a safe plant based antimicrobial against fungal and aflatoxin B1 contamination of spices, *Food Res. Int.*, 2011, **44**(1), 385–390.

14 R. P. Adams, *Identification of Essential Oil Components by Gas Chromatography/mass Spectrometry*, Gruver, TX USA, Texensis Publishing, 5th edn, 2017.

15 M. Beyki, S. Zhaveh, S. T. Khalili, T. Rahmani-Cherati, A. Abollahi, M. Bayat, M. Tabatabaei and A. Mohsenifar, Encapsulation of Mentha piperita essential oils in chitosan–cinnamic acid nanogel with enhanced antimicrobial activity against Aspergillus flavus, *Ind. Crops Prod.*, 2014, **54**, 310–319.

16 S. F. Hosseini, M. Zandi, M. Rezaei and F. Farahmandghavi, Two-step method for encapsulation of oregano essential oil in chitosan nanoparticles: Preparation, characterization and *in vitro* release study, *Carbohydr. Polym.*, 2013, **95**(1), 50–56.

17 A. Kujur, A. Kumar, P. P. Singh and B. Prakash, Fabrication, characterization, and antifungal assessment of jasmine essential oil-loaded chitosan nanomatrix against Aspergillus flavus in food system, *Food Bioprocess Technol.*, 2021, **14**, 554–571.

18 B. Prakash, P. Singh, P. K. Mishra and N. K. Dubey, Safety assessment of Zanthoxylum alatum Roxb. essential oil, its

antifungal, antiaflatoxin, antioxidant activity and efficacy as antimicrobial in preservation of Piper nigrum L. fruits, *Int. J. Food Microbiol.*, 2012, **153**(1–2), 183–191.

19 J. Tian, B. Huang, X. Luo, H. Zeng, X. Ban, J. He and Y. Wang, The control of Aspergillus flavus with Cinnamomum jensenianum Hand.-Mazz essential oil and its potential use as a food preservative, *Food Chem.*, 2012, **130**(3), 520–527.

20 G. A. Helal, M. M. Sarhan, A. N. Abu Shahla and E. K. Abou El-Khair, Effects of Cymbopogon citratus L. essential oil on the growth, morphogenesis and aflatoxin production of Aspergillus flavus ML2-strain, *J. Basic Microbiol.*, 2007, **47**(1), 5.

21 M. P. Singh, Application of Biolog FF MicroPlate for substrate utilization and metabolite profiling of closely related fungi, *J. Microbiol. Methods*, 2009, **77**(1), 102–108.

22 A. Kedia, B. Prakash, P. K. Mishra, A. K. Dwivedy and N. K. Dubey, Biological activities of Cuminum cyminum seed oil and its major components against Callosobruchus chinensis and Sitophilus oryzae, *J. Asia-Pac. Entomol.*, 2015, **18**(3), 383–388.

23 B. Prakash, A. Kedia, P. K. Mishra and N. K. Dubey, Plant essential oils as food preservatives to control moulds, mycotoxin contamination and oxidative deterioration of agri-food commodities–Potentials and challenges, *Food Control*, 2015, **47**, 381–391.

24 A. Kujur, A. Kumar, A. Yadav and B. Prakash, Antifungal and aflatoxin B1 inhibitory efficacy of nanoencapsulated Pelargonium graveolens L. essential oil and its mode of action, *Lwt*, 2020, **130**, 109619.

25 V. Rajkumar, C. Gunasekaran, C. A. Paul and J. Dharmaraj, Development of encapsulated peppermint essential oil in chitosan nanoparticles: Characterization and biological efficacy against stored-grain pest control, *Pestic. Biochem. Physiol.*, 2020, **170**, 104679.

26 Y. Xu, H. Chen, L. Zhang and Y. Xu, Clove essential oil loaded chitosan nanocapsules on quality and shelf-life of blueberries, *Int. J. Biol. Macromol.*, 2023, **249**, 126091.

27 M. Mondéjar-López, A. Rubio-Moraga, A. J. López-Jimenez, J. C. Martínez, O. Ahrazem, L. Gómez-Gómez and E. Niza, Chitosan nanoparticles loaded with garlic essential oil: A new alternative to tebuconazole as seed dressing agent, *Carbohydr. Polym.*, 2022, **277**, 118815.

28 B. R. Rizeq, N. N. Younes, K. Rasool and G. K. Nasrallah, Synthesis, bioapplications, and toxicity evaluation of chitosan-based nanoparticles, *Int. J. Mol. Sci.*, 2019, **20**(22), 577.

29 M. Payandeh, M. Ahmadyousefi, H. Alizadeh and M. Zahedifar, Chitosan nanocomposite incorporated Satureja kermanica essential oil and extract: Synthesis, characterization and antifungal assay, *Int. J. Biol. Macromol.*, 2022, **221**, 1356–1364.

30 A. Kumar, P. P. Singh and B. Prakash, Unravelling the antifungal and anti-aflatoxin B1 mechanism of chitosan nanocomposite incorporated with Foeniculum vulgare essential oil, *Carbohydr. Polym.*, 2020, **236**, 116050.

31 A. Yadav, A. Kujur, A. Kumar, P. P. Singh, V. Gupta and B. Prakash, Encapsulation of Bunium persicum essential oil using chitosan nanopolymer: Preparation, characterization, antifungal assessment, and thermal stability, *Int. J. Biol. Macromol.*, 2020, **142**, 172–180.

32 F. Donsì, M. Annunziata, M. Sessa and G. Ferrari, Nanoencapsulation of essential oils to enhance their antimicrobial activity in foods, *LWT–Food Sci. Technol.*, 2011, **44**(9), 1908–1914.

33 W. Liao, W. Badri, E. Dumas, S. Ghnimi, A. Elaissari, R. Saurel and A. Gharsallaoui, Nanoencapsulation of essential oils as natural food antimicrobial agents: An overview, *Appl. Sci.*, 2021, **11**(13), 5778.

34 Y. Wang, J. Xu, W. Lin, J. Wang, H. Yan and P. Sun, Citral and cinnamaldehyde–Pickering emulsion stabilized by zein coupled with chitosan against Aspergillus. spp and their application in food storage, *Food Chem.*, 2023, **403**, 134272.

35 R. Karami-Osboo, M. Mahboubifar, M. Mirabolfathy, L. Hosseinian and A. R. Jassbi, Encapsulated Zataria multiflora's essential oil inhibited the growth of Aspergillus flavus and reduced aflatoxins levels in contaminated pistachio nut, *Biocatal. Agric. Biotechnol.*, 2023, **51**, 102796.

36 L. M. Douglas and J. B. Konopka, Fungal membrane organization: the eisosome concept, *Annu. Rev. Microbiol.*, 2014, **68**, 377–393.

37 S. Dhingra and R. A. Cramer, Regulation of sterol biosynthesis in the human fungal pathogen Aspergillus fumigatus: opportunities for therapeutic development, *Front. Microbiol.*, 2017, **8**, 92.

38 S. Basak and P. Guha, A review on antifungal activity and mode of action of essential oils and their delivery as nano-sized oil droplets in food system, *J. Food Sci. Technol.*, 2018, **55**, 4701–4710.

39 W. Chen, T. Xie, Y. Shao and F. Chen, Phylogenomic relationships between amylolytic enzymes from 85 strains of fungi, *PLoS One*, 2012, **7**(11), e49679.

40 A. Kumar, P. P. Singh and B. Prakash, Assessing the efficacy of chitosan nanomatrix incorporated with Cymbopogon citratus (DC.) Stapf essential oil against the food-borne molds and aflatoxin B1 production in food system, *Pestic. Biochem. Physiol.*, 2022, **180**, 105001.